

Thermomechanics of Laser-Induced Shock Waves in Combustible Mixtures

Nathan D. Peters, Deshawn M. Coombs, and Ben Akih-Kumgeh
Syracuse University
Syracuse, NY, USA

1 Introduction

Laser ignition has drawn considerable interest as a replacement for spark plug ignition due to its ability to improve lean-burn engine performance. Implementation of this technology is hindered by the complex multiphysics nature of the problem. Above a certain threshold, a laser being focused on a small volume can cause optical breakdown forming a high temperature plasma. Given the relatively short energy deposition time compared to the acoustic time, the pressure builds up, coalescing into a shock wave. If these processes occur in reactive mixtures, the high temperature near the focal region will eventually initiate a self-sustained combustion wave. In order to simulate such forced ignition events, we must have a detailed understanding of the fundamental processes of the problem. A thorough investigation of the thermomechanics of the laser-induced shock wave can provide insight about the thermodynamic conditions prior to flame kernel formation. Since it is possible to describe the shock dynamics using a blast wave theory, estimates can be made of the proportion of absorbed energy used for the shock wave generation. The shock wave investigation is the first step in our ongoing study of the laser ignition process.

As the need for detailed laser ignition models has increased, so has the number of studies focusing on laser-induced shock waves. Navarro-Gonzalez et al. [1] investigated shock waves formed by 1.064 μm laser pulse in 1 atm of air. The shock radius at a given time was found not to have a strong dependence on focal length. In a separate study by the same authors [2], the average shock velocity for a 300 mJ pulse was found to be 460 ± 70 m/s at 1 μs . The shock velocity for a 300 mJ pulse in air was also investigated by Lackner et al. [3]. They found a much higher velocity of 1,900 m/s at 1 μs showing that there are still a lot of inconsistencies in shock velocity measurements among different research groups. They also looked at reactive cases such as methane ignition, showing that equivalence ratio had a negligible effect on the size of the initial ellipsoidal flame kernel. Recently, Gebel et al. [4] compared experimental shock velocity results to numerous blast wave theories. They found that the often referenced Taylor-Sedov blast theory [5] does not work for laser-induced shock waves since the Mach number quickly reduces to unity. It was also found that more than 50% of the energy from the absorbed laser pulse can go to generating the shock wave.

Despite a growing number of studies focusing on laser ignition, there are still many gaps in our understanding, partly due to challenges in high temporal resolution. During the earliest stages of ignition, broadband bremsstrahlung emissions hinder observation access to the absorbing gas volume. At later times, the shock wave and other processes happen quickly, leading to difficulties in obtaining time-resolved data. To resolve these problems, experiments should be complemented by computational fluid dynamic (CFD) simulations which can probe time-scales otherwise unobtainable through experiments. With knowledge of the energy used to generate the shock wave and the geometry of the receiving volume, CFD analysis can provide insight into the early behavior of the plasma and subsequent flame kernel.

This paper presents a combined experimental and CFD study of laser-induced shock waves. Optical breakdown is induced using a Nd:YAG laser at 3 different energy levels in air, methane, and biogas mixtures. The experimental results of breakdown in air are then compared with simulations, providing further insight into the behavior of the shocked gas.

2 Experiment and Simulation Methodology

2.1 Experimental Setup

Experiments are carried out in a cylindrical combustion chamber with optical access on six sides. Sapphire windows on the side walls provide access for the focused laser light and end wall quartz windows are used for imaging diagnostics. The chamber is 15.24 cm in diameter and 25.4 cm long. Compressed gases are supplied to the chamber through a central manifold. Mixture preparation is by the method of partial pressures using a mounted pressure transducer. This project investigates breakdown in air, methane/N₂, methane/air, and biogas/air. Fuels are added first, followed by oxygen, then nitrogen. Gases are allowed to mix before the experiment begins. The biogas is a composition of 60% methane and 40% CO₂.

Breakdown of gas mixtures is induced by a Spectra-Physics 10 Hz Nd:YAG laser at 532 nm with a pulse duration of 8 ns. Laser energy is measured in two locations using power meters (Ophir PE-25), as shown in Figure 1. One power meter determines the incident energy from a portion of the beam deflected by a variable attenuator. The incident energy from the laser is controlled by adjusting the variable attenuator. The other power meter is placed behind the chamber to determine the residual energy after breakdown or ignition. The energy absorbed by the gas within the chamber is determined by subtracting the residual energy from the incident energy. The laser energies recorded by the power meters are corrected by taking into account losses through the sapphire windows and focusing optics. To ensure accuracy of the energy readings, the chamber is vacuumed out before each test and the laser is pulsed to guarantee nearly 100% transmission.

Schlieren images are recorded with a high speed camera (Photron SA-4). A LED light source is focused through an iris and collimated between two 50 cm focal length mirrors in Z-type configuration. All data acquisition and process control are done using a computer program. The camera is triggered by a digital delay generator (SRS DG-645) that is timed with the laser pulse. Due to limitations in camera speed, one image was recorded per breakdown event. The incident laser energy was kept within $\pm 3\%$ from shot to shot providing good reproducibility. The delay between the laser pulse and camera trigger was gradually increased from 2 to 10 μs . The schlieren images were processed utilizing an edge detection algorithm in Matlab. From the processed images, the shock radius was measured vertically from the center of the plasma to the edge of the shock front. Three sources of uncertainty for the shock wave radius measurements are accounted for by the error bars on the experimental data: (1) variability in the laser deposition energy (2)

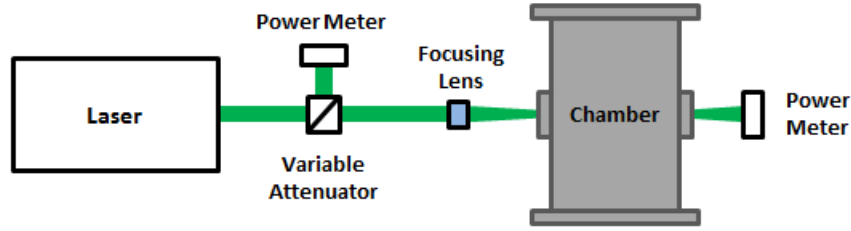


Figure 1: Experimental setup depicting the arrangement of laser power meters for measuring incident and absorbed laser pulse energies.

errors due to scaling of the shock wave images and location of the shock front as determined by the Matlab code and (3) time delays in the triggering and camera equipment.

2.2 Analysis of Experimental Results

From the sequence of images at a given pulse energy, a temporal evolution of the shock front is obtained. One would like to deduce the energy required to reproduce this shock trajectory. Gebel et al. [4] recently showed that for laser-induced shock waves in air, the blast wave model by Jones [6] more accurately predicts the shock radius than the often used Taylor-Sedov blast wave theory. This is especially true for times greater than $1 \mu\text{s}$ when the Mach numbers are less than 2. Using Equation 1 and experimentally obtained shock radii, a least-squares method can be used to determine the initial energy, E_0 , which best fits the data.

$$\tau = 0.543 \left[\left(1 + 4.61x(t)^{5/2} \right)^{2/5} - 1 \right] \quad (1)$$

Where τ and $x(t)$ are non-dimensional quantities such that:

$$\tau = c_0 \frac{t}{r_0} \quad \text{and} \quad x(t) = \frac{r(t)}{r_0}; \quad \text{with} \quad r_0 = \left[\frac{6.25E_0}{B\gamma p_0} \right]^{1/3}$$

Here, t is the dimensional time, r is the radius, r_0 is the reference radius, c_0 is the speed of sound, γ is the ratio of specific heats, p_0 is the pressure of the undisturbed gas, and B is a geometry parameter. The equations to calculate B are given in [7] and are functions of the ratio of specific heats, γ . From a given fit, the corresponding E_0 can be used to simulate the shock.

2.3 Simulation Methodology

To complement experimental studies, the Navier-Stokes equations are used to simulate the flow field developed by the deposition of laser energy in gases. Several studies of laser induced plasma in air have involved the numerical simulation of the flow field developed. Dors and Parigger [8] studied the gas dynamic effects and the kernel dynamics after breakdown. The roll up of the plasma core was explored by Ghosh and Mahesh [9]. Radiation loss from the decaying core in air was investigated by Joarder et al. [10].

In the present simulations the Navier-Stokes equations in integral form are solved using the commercial software Star-CCM+. The Navier-Stokes equation in vector form can be written as follows,

$$\frac{\partial \mathbf{U}}{\partial t} + \frac{\partial}{\partial x_j} (\mathbf{F}_j^c - \mathbf{F}_j^v) = \mathbf{S} \quad (2)$$

where \mathbf{U} is the vector of conservative variables, \mathbf{S} the source term vector, and \mathbf{F}_j^c and \mathbf{F}_j^v the inviscid and viscous flux terms. The solution is first order in time and is second order in space in smooth regions. The inviscid flux terms are discretized using the approximate Riemann solver by Roe. In addition, oscillations are controlled by use of the Venkatakrisnan limiter.

The number of equations to be solved depends on the relevant physics model of the problem. In the present simulations the plasma is assumed to be in local thermodynamic equilibrium, and the gas is modeled using the ideal gas model. Chemical reactions in the plasma kernel due to high temperatures have been neglected in these simulations, as well as radiation transfer effects. The transport properties are modeled using power law descriptions, and the specific heat is modeled using a polynomial equation. Due to the approximate symmetric shape of the resulting plasma a 2D simulation can be adopted. These assumptions lead to no extra source terms and the following expressions,

$$\mathbf{U} = (\rho, \rho u_i, \rho e)^T; \quad (3)$$

$$\mathbf{F}_j^c = (\rho u_i, \rho u_j u_i + p \delta_{ij}, u_j (\rho e + p))^T \quad (4)$$

$$\mathbf{F}_j^v = (0, \tau_{ij}, u_i \tau_{ij} + q_{ij})^T; \quad (5)$$

The initial plasma is of a rectangular shape, and pressure and temperature conditions of the plasma are assumed to be constant over the volume. The focal volume used to initialize the simulation is $3.66 \times 10^{-3} \text{ mm}^3$, calculated using optical theory [11]. Blast wave energies obtained from experimental results are used to calculate increases in temperature and pressure that a mass of gas within the focal volume would experience due to the deposited energy. The computations are carried out on a domain of $25 \times 12.5 \text{ mm}$ and discretized into half a million computational cells.

3 Results and Discussion

The experimentally determined point blast energies of the laser-induced shock waves for various mixtures are shown in Table 1 for three different absorbed energies. For the 12.2 mJ of absorbed energy in air, the shock wave showed a point blast energy of 9.9 mJ which constitutes 81% of the absorbed energy by the gas. This shows reasonable agreement with Gebel et al. [4] who reported blast wave energy that is 77.7% of 11.6 mJ absorbed energy in air. An inert mixture of methane and nitrogen showed very similar blast wave energies to air, while reactive mixtures all showed higher blast wave energies. This is likely due to the additional energy released from the fuel in the vicinity of the focal region. Both lean methane/air and biogas mixtures produced lower blast wave energies than the stoichiometric methane/air mixture, showing that composition of the gas plays an important role even very early on in the ignition process.

For the case of laser-induced shock waves in air, the experimentally determined shock radii are compared with the simulation results in Figure 2 for all three absorbed energy levels investigated in this study. In general, the simulation results agree well with the experimental data. As this study continues, focal volume

Table 1: Point blast energies calculated using Jones blast wave theory compared to absorbed laser energy in mixtures at $p = 1 \text{ atm}$, $T = 300 \text{ K}$.

Absorbed Energy	Air	Methane/N2	Methane/Air Stoichiometric	Methane/Air Lean	Biogas/Air Stoichiometric
$25.2 \pm 0.5 \text{ mJ}$	22.4 mJ	22.6 mJ	25.5 mJ		24.7 mJ
$12.2 \pm 0.3 \text{ mJ}$	9.9 mJ		11.2 mJ	10.6 mJ	
$3.8 \pm 0.15 \text{ mJ}$	3.4 mJ		4.5 mJ	4.0 mJ	

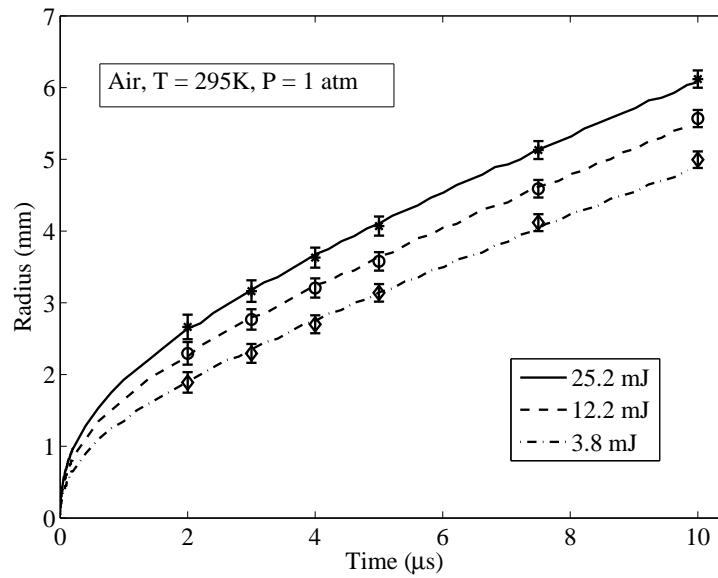


Figure 2: Comparison of laser induced shock wave radius from experiment (symbols) and simulation (line).

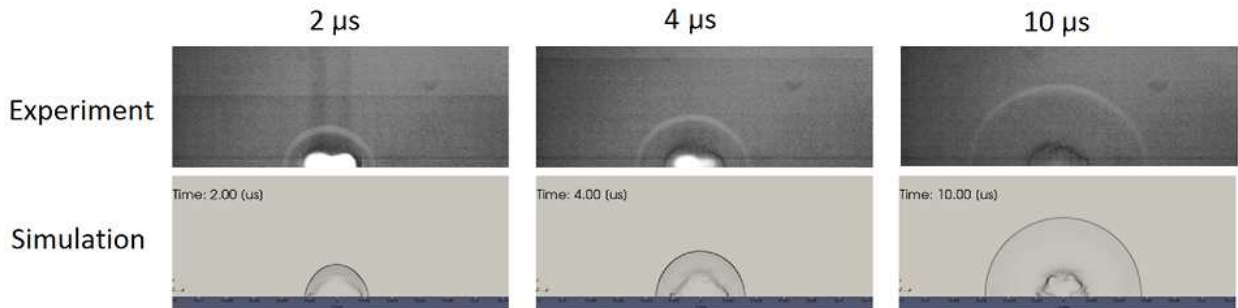


Figure 3: Schlieren images (top) of the laser induced shock evolution compared with density gradient contours from the simulation (bottom). Absorbed energy is 25.2 mJ.

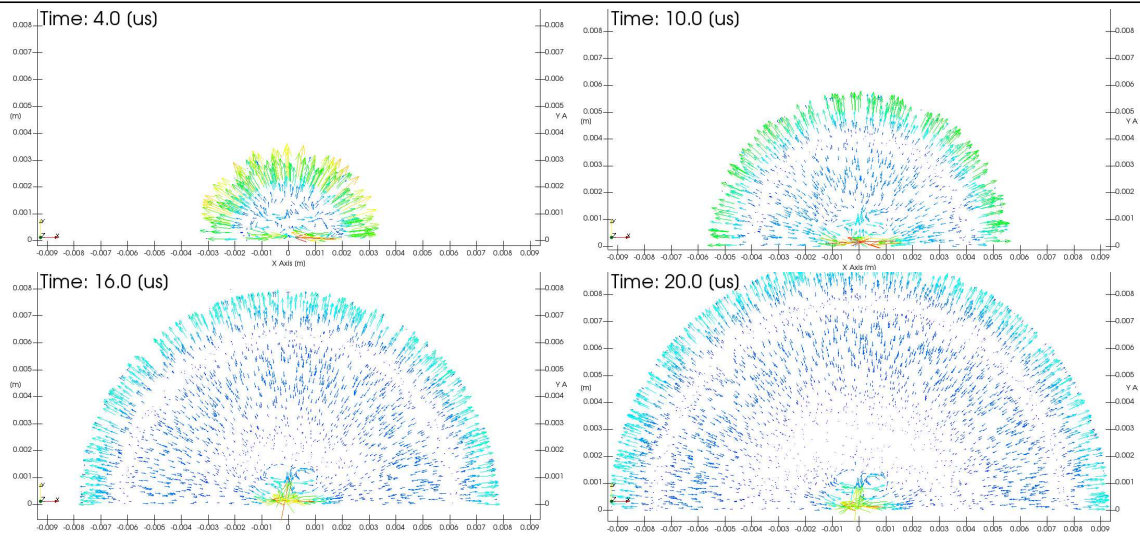


Figure 4: Evolution of velocity field.

geometry and radiative heat loss will be considered to determine if these factors contribute to the differences in shock trajectory.

Schlieren images of air breakdown are compared with the density gradient from the simulation for 25.2 mJ in Figure 3. At the same time instants, the simulation shows a blast wave encompassing a similar volume that seen in the experimental results, consistent with the results from Figure 2. The temporal evolution of the blast waves are quite similar, as expected from the shock wave radius results. Schlieren imaging provides limited information about what occurs in the hot core at the center of the blast wave. The simulation results allow for insight into quantities such as temperature and velocity fields. The development of the velocity field obtained through the simulation is shown in Figure 4. After the breakdown event, a region of low density originating from the focal volume expands with the shock wave. As the shock wave progresses, it detaches from the low density hot core which then collapses inducing vortices near the center of the shocked region. The formation of these vortices that can be seen at 16 and 20 μs in Figure 4.

4 Conclusion

Laser-induced shock waves in air, methane/ N_2 , methane/air, and biogas/air have been investigated, complemented by CFD simulations. The mechanics of the resulting shock waves can be properly captured using the blast wave theory by Jones, from which energies required for shock generation can be estimated. The blast wave energies showed gas composition plays an important role very early in the breakdown process. For the case of breakdown in air, the CFD simulations generally accord with experimental observations. The simulated flow field also reveals velocity and vorticity patterns within the shocked region.

References

- [1] R. Navarro-Gonzalez and M. Villagran-Muniz, "Effect of beam waist on shock properties of laser-induced plasmas in air by the photoacoustic probe beam deflection method," *Analytical Sciences*,

- vol. 17, pp. 118–121, 2001.
- [2] M. Villagran-Muniz, H. Sobral, and R. Navarro-Gonzalez, “Shock and thermal wave study of laser-induced plasmas in air by the probe beam deflection technique,” *Measurement Science and Technology*, vol. 14, pp. 614–618, 2003.
- [3] M. Lackner, S. Charareh, F. Winter, K. F. Iskra, D. Rdisser, T. Neger, H. Kopecek, and E. Wintner, “Investigation of the early stages in laser-induced ignition by schlieren photography and laser-induced fluorescence spectroscopy,” *Optics Express*, vol. 12, pp. 4546–4557, 2004.
- [4] G. C. Gebel, T. Mosbach, W. Meier, and M. Aigner, “Laser-induced blast waves in air and their effect on monodisperse droplet chains of ethanol and kerosene,” *Shock Waves*, vol. 25, pp. 415–429, 2015.
- [5] G. Taylor, “The formation of a blast wave by a very intense explosion,” *I. Theoretical discussion. Proc. R. Soc. Lond. A*, vol. 201, pp. 159–174, 1950.
- [6] D. L. Jones, “Intermediate strength blast wave,” *Physics of Fluids*, vol. 11, 1968.
- [7] D. Jones, “The energy parameter b for strong blast waves,” *Ntl. Bureau of Stds. Tech. Note*, vol. 155, 1962.
- [8] I. Dors and C. G. Parigger, “Computational fluid dynamic model of laser induced breakdown in air,” *Applied Optics*, vol. 42, 2003.
- [9] S. Ghosh and K. Mahesh, “Numerical simulation of laser induced breakdown in air,” *46th AIAA Aerospace Sciences Meeting and Exhibit*, 2008.
- [10] R. Joarder, G. C. Gebel, and T. Mosbach, “Two-dimensional numerical simulation of a decaying laser spark in air with radiation loss,” *Int. J. Heat and Mass Transfer*, vol. 63, pp. 284–300, 2013.
- [11] J. Stricker and J. G. Parker, “Experimental investigation of electrical breakdown in nitrogen and oxygen induced by focused laser radiation at 1.064,” *Journal of Applied Physics*, vol. 53, pp. 851–855, 1982.